Using Direct Printing Technologies to Reproduce Very Fine Conductive Traces on Paper

Bemly Randeniya*, Dr. Howard E. Nelson**, Dr. William J. Ray*

Abstract

The term "printed electronics" is used to describe the use of a method of printing to create electrically functional devices (Blayo and Pineaux, 2005). Since the inception of the printed circuit, printing processes have offered circuit board manufacturers an inexpensive method to mass-produce circuit boards that were accurate, standardized, and functional. Yet printed electronics faces several challenges. One of these is the accurate printing of a thin conductive line. There are numerous critical material characteristics that play a significant role in the capability of the printing processes including conductive inks, dielectric substrates with smooth surfaces, and print resolution.

Typically, print resolutions during optical printing may achieve resolutions as low as 8 µm during the transfer of halftone color images, if one considers the smallest size of a discrete halftone dot. In any printing process there are specific requirements that must be met in order to achieve the best possible print quality. These include the accuracy of the permanent master, ink transfer mechanism pressure, impression pressure, and press speed. When considering printed electronics, achieving a printed line resolution that facilitates electronic capacity and mobility is the foremost challenge.

The human eye is capable of distinguishing objects as small as 25 microns. Thus, both the gravure process and the flexographic process are designed to reproduce at this resolution. For the printing of electrical circuitry, the appropriate electrical functionality can be achieved by a series of 25-µm line widths, separated by 25-µm non-conductive spaces (Hagberg, Pudas, Leppävuori, Elsey, and Logan, 2002).

The objective of this study is to analyze the advantages and limitations of manufacturing electronic components using the printing process, while comparing the fine-line printability between the gravure and flexographic printing processes, while considering the limitations of ink, substrate, and processes.

*NthDegree Technologies, Tempe, Arizona, USA
**Arizona State University, Mesa, Arizona, USA

Introduction

The term "printed electronics" is used to describe the use of printing processes to create electrically functional devices (Blayo and Pineaux, 2005). Since the 1950s, the printing processes have offered the circuit board manufacturing industry an inexpensive method to mass-produce printed circuit boards that were accurate, standardized, and functional. Early printed circuit boards (PCBs) were printed using the screen-printing process to lay conductive traces on a non-conductive support such as phenolic or epoxy plastic, using conductive inks to lay the circuit path on the substrate (Sheets, 2004). These early PCBs could be laminated to other materials creating the di-electric hybrid circuit needed for complex component assembly.

In those early days, paper was often considered for use as a substrate due to its ready availability, beneficial electrical properties, and low cost. It was rejected by the process considerations of the time because of its rough surface, its tendency to absorb liquids, and its vulnerability to other materials such as liquid plastics and solder (Harrey, 2000). In place of paper, plastics and structured silicon have been used more widely as substrates, especially as fabrication technology progressed. This is largely due to the substandard functional performance of printed electronics when compared to conventionally packaged electronic components. While applications that require high switching frequencies and high integration density in board packaging will continue to be dominated by conventional components-on-board electronics in spite of its high design and fabrication costs, printed electronics as a complementary technology can lead to low-cost fabrication for emissive applications and have the potential to replace conventional electronic fabrication methods for functional products (Falchetti, 2007).

Additionally, as thin-film chemistry has progressed, printed electronics has become associated with the use of organic inks that are composed of carbon-based compounds utilizing soluble chemical carriers to image the material. These carbon-based fluid carriers allowed researchers to use multiple printing processes in imaging the substrates in order to optimize performance and production costs (Xu, 2000). According to Gupta (2000), the use of multiple processes holds the promise that printed electronic production might become process-agnostic, using the best process for a particular application and multiple processes as discrete printing cassettes in the same production press.

Similar to conventional optical-based printing where multiple ink layers are printed on top of one another, electronic thin-film devices are made by printing several functional layers on top of each other. Understandably, both the materials used in printed electronics and the requirements of the properties of the printed functional layers differ from the visual image. This made the repurposing of printing technologies the most essential task in the development

and production of printed electronic products. To date, several printing processes were piloted by printing them utilizing common printing equipment from the graphics arts industry, such as screen printing, flexography, gravure, dry-offset lithography, inkjet, and scrape application (Bock et al., 2005).

In the same technological period as advancements were occurring in print technology, the paper manufacturing industry was also discovering and using new technology in the manufacture of its product. Coatings have made substantial progress, resulting in paper substrates that have a range of coating applications, available to the end user for different applications. For the first time, the availability of many of these modern coating processes made the use of paper as a substrate in printed electronics viable (Moore, 2004). These low-cost substrates proved ideal for the very low-cost, limited-use electronics intended for applications not typically associated with silicon-based electronics, such as lighted packaging, smart labels, or animated point-of-purchase display products.

With these high-tech coatings, modern paper appeared capable of producing the resolutions demanded by printed electronics. In the more conventional optical-based printed product, the minimum required graphic design resolution was determined by the ability of human vision to distinguish each discrete design feature. The unaided human eye is generally incapable of distinguishing individual design components that were sized below 25 µm.

Product Requirements

As printed electronics evolved, it became apparent that 25 µm was similar in width to conductive traces in a printed circuit and likewise needed an equivalent sized non-conductive space between traces in order to influence the integration density of the printed circuit and contribute to the functionality of added devices such as transistors, routers, and capacitors. Similar tolerances also existed for the precision with which layers are printed on top of one another (i.e., layer to layer registration). In that era, the 25-µm trace dimension target was also considered the dimension at which the layer registration, the prevention of pin-holes in the trace, and control of the mechanical growth of the printed image in the application can be optimally obtained (Hagburg, Leppavuori, Elsey, and Logan, 2002). In printed electronics for signage and packaging, an expanded range of materials must be processed in the manufacture, which required new levels of compatibility of the printed layers regarding adhesion, wetting, dissolving, and the registration of the optically recognized printed image with the electronic display field (Gamota, Brazis, Kalyanasundaram, and Zhang, 2004).

When compared to modern traditional microelectronics, printed electronics hold the promise of being able to produce a directly functional product with specific properties, using a manufacturing technique that is both flexible and cost-effective. Among the advantages of printed electronics are low design and

production costs; rapid turnaround of orders; flexible substrates such as film, foils, and papers; light weight; and improved environmental credentials.

Though promising in production terms, producing printed electronics has challenges in several areas. The accurate, consistent reproduction of a very-thin and continuously conductive trace is not the least of them. Achieving a very-thin trace that has acceptable conductivity with the printing of conductive inks is a major challenge of printed electronics. Line resolution is critical, and problems of line breaks and fill-in of blank non-conductive spaces are inherent in this type of manufacturing. If the objectives of low cost and high volume in manufacturing are important to the use of printed electronics, one or more of the high-volume print processes will have to be adapted to manufacture these goods.

With high-volume print, there are numerous critical material characteristics that play a significant role as they interact with parts of the printing process. This list includes the function of conductive inks, the required thickness of the ink film deposit on the substrate, the ink resin topology including the ink filler content, the roughness of the substrate's surface, and the minimum allowable print resolution needed to print the conductive traces. Added to this are the operational considerations involved in making the ink transfer occur in the printing cassette, such as the ink surface tension, the ink viscosity, and the electrical continuity of the printed result (Vardeny, 2005). As processes are scaled up to produce more product and bring manufacturing costs down, we can predict that printed electronics will be produced in quantity using high-speed printing technology.

Purpose of the Research Project

The purpose of this project was to examine the fine-line resolution capabilities of two of the high-speed printing processes for use in manufacturing Printed Thin Film (PTF) circuit boards. In order to achieve success, very thin, homogeneous, and defect-free layers of semiconductor materials, dielectric materials, and gate electrodes must be deposited onto a substrate as accurately as possible (Gamota, Brazis, Kalyanasundaram, and Zhang, 2004, p. 178).

One of the important promises of PTF technology is the ability to produce a variety of high-speed electrical components. In conventional hybrid microelectronic screen printing technology, the printing accuracy limit is about 150 μm in high-volume production. The tendency of PTF technology towards smaller and more efficient electrical equipment required both higher packing density and smaller dimensions for components and interconnection substrates. Thus, for high-speed circuitry, the quality and dimensions of the electrical interconnecting lines became even more important (Hagberg, Pudas, Leppävuori, Elsey, and Logan, 2002).

The function of a printed circuit board (PCB) is to connect a variety of active components (such as microchips and transistors) and passive components (such as capacitors and fuses) into an electronic assembly that controls a system. A typical PCB consists of conductive "printed wires" attached to a rigid, insulating "board." The insulating board is often called the substrate (National Research Council, 2005). We used this series of experiments to verify the belief that TFP technology offered the manufacturing advantages we sought.

We focused our efforts on the analysis of both the flexographic process and the gravure process in relationship to their ability to print the ultra-fine lines necessary for printed electronics using conductive inks. These experiments used paper as the flexible substrate. The paper used for this test for both processes was Lusterprint GR2Max (81 gsm) which was treated with a Fluoro-chemical normally used in the manufacture of fertilizer bags. The ink used for both processes was Electrodag PE 003 from Acheson Colloids, which is a single-fluid, carbon-based conductive ink.

Research Objectives

The first research effort was to develop a suitable digital test pattern in order to make flexographic plates and engraved gravure cylinders. The second objective was to analyze the final printed pieces and all the variables associated with these experiments. The third and final objective was to compare the ultra-fine-line printability using particulate conductive inks for both the flexographic and gravure printing processes. The following experiments were carried out to achieve the three objectives listed above:

1. Developed a common suitable digital fine-line test pattern to image both flexographic plates and engrave gravure cylinders.
2. Imaged plates and cylinder with the test pattern image and verified that the engraving or image transfer methods reproduced the test pattern accurately.
3. Conducted porosity and surface smoothness tests for the substrate.
4. Carried out a surface energy analysis of the paper substrate and an overall surface tension on the conductive ink and made contact angle measurements of the conductive ink.
5. Printed the test pattern using the inks and substrate combination chosen for the experiment with both printing processes, while taking care to minimize the process variation during printing.
6. Made a microscopic evaluation of the printed sheets to determine the extent of the mechanical growth and directional characteristics of the printed lines.
7. Carried out a Thermo Gravimetric Analysis (TGA) and evaluated the filler content of conductive ink samples.
8. Measured the conductivity of fine lines for different resolution patches.

9. Evaluated the adhesion of the printed test pattern to the substrate with a standard ASTM tape test.

Scope of the project

This study basically is focused on the performance of two printing processes, flexography and gravure, relating to achieving ultra-fine-line printing using conductive inks. The experiments were conducted to determine whether the quality of the printed line via one of the processes was better than the quality of the other. Since the two processes have their inherent constraints on ink transfer, the same fluid ink was chosen to use for both printing processes.

EXPERIMENTS & RESULTS

Test Patterns

Given press limitations such as plate size and web width, the test pattern was created by the researchers to evaluate the resolution of the printing system for both processes. The flexo digital test print pattern was prepared at 2400-ppi resolution in bitmap mode using Adobe Photoshop. The gravure test pattern was created at 4800-ppi resolution in bitmap mode to achieve the maximum fidelity of the engraved lines. The same test pattern in each resolution was run using both the flexo and gravure printing processes respectively.

The test pattern can be described as consisting of eight different line resolutions (600 lpi, 400 lpi, 300 lpi, 200 lpi, 150 lpi, 120 lpi, 100 lpi, and 80 lpi). Please note that lpi (lines per inch) used for printed electronics were not the same as the resolution for the print media. For calculating resolution in terms of traces, void (non-printed) lines are also considered in the lines-per-inch amount (hence, the resolution in print media terms is equal to one-half the stated resolution, e.g., 100 lpi in this paper = 50 lpi in printing terms).

Each line pattern was used with vertical and horizontal alignment and equal line width as well as equal void spacing. Line widths were measured for the above sequence as 42 μm, 63 μm, 84 μm, 127 μm, 169 μm, 211 μm, 254 μm, and 317 μm respectively. Another set of lines were also included in the same resolution but with a fixed width. The fixed width was selected as 2 px, which is approximately 21.17 μm at 2400-dpi resolution. Each set of lines in the same resolution was placed in adjacent columns (see Figure 1).

The second artwork series was created using the same line resolution, but respective sets of horizontal and vertical lines at the same resolution were placed one above the other (see Figure 2). Subsequently these test patterns were used in the final artwork as Target 1A and Target 1B respectively.

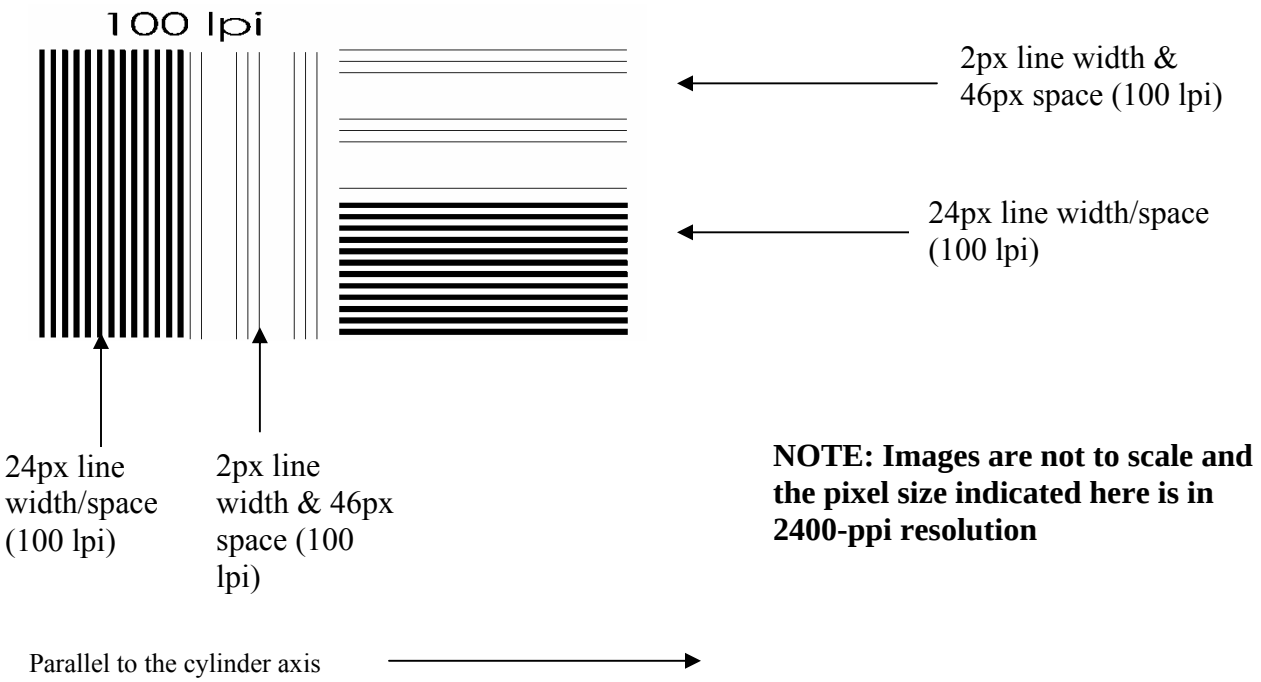

Figure 1. *Both horizontal and vertical line patterns in the same resolution were placed in adjacent columns.*

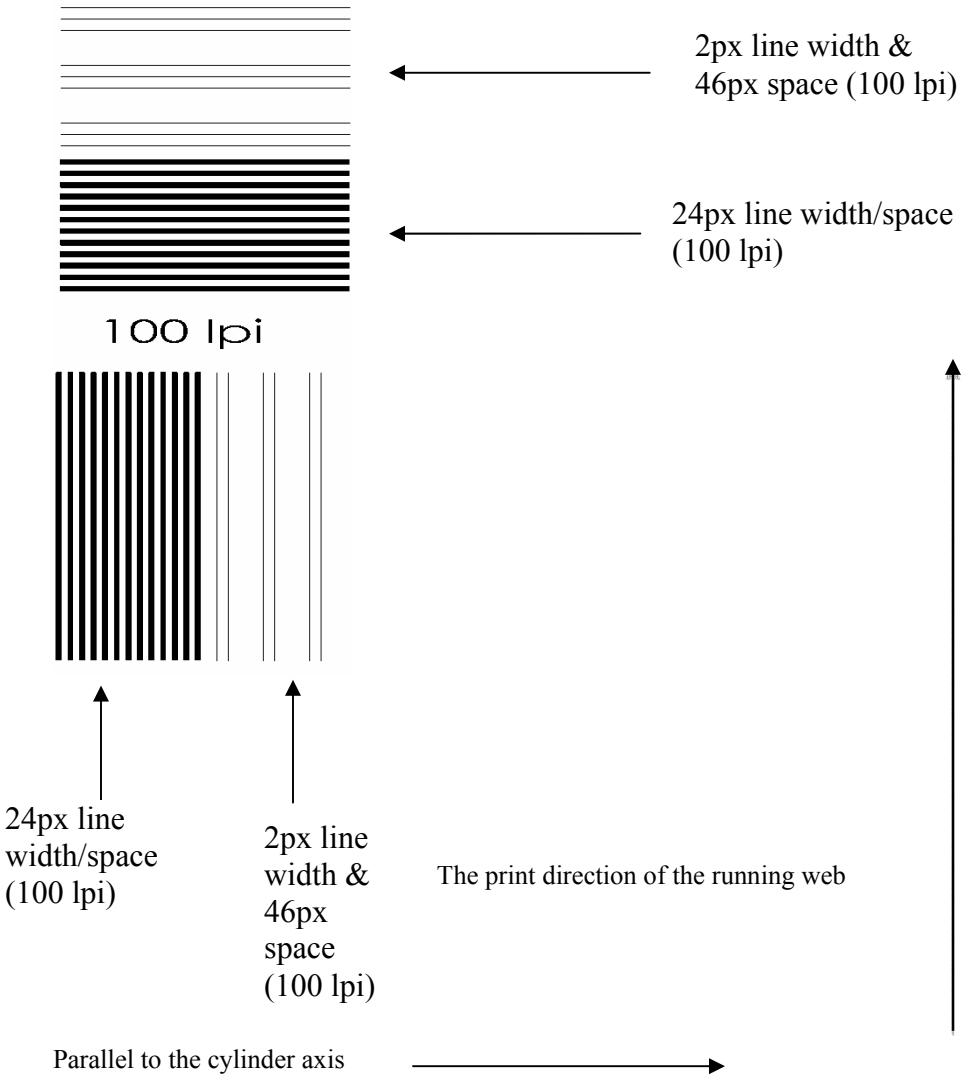

Figure 2. *Both horizontal and vertical line patterns in the same resolution were placed in the same column, one above the other, in order to compare lines in the print direction to lines across the print direction.*

Digital artwork

Five different test patterns described below were part of the final artwork (see Figure 3). The Sheppers Digilas engraver is capable of reproducing very high-resolution digital files, and the researchers found it more suitable to use the

4800-ppi file in order to avoid the stair-step-contour effect along curved edges in gravure process.

The final artwork was comprised of blocks of lines as shown in Target 1A, and blocks of lines as shown in Target 1B. Further, three columns also were included as described below:

1. Target 2A was comprised of 80-lpi, 100-lpi, 120-lpi, and 150-lpi resolution line patches in press directional and cross press directional position respectively. In the same target, the constant width 21.17-μm target in 100-lpi resolution was placed adjacent to each of the four resolutions above.
2. Target 2B was in column format and was comprised of 100-lpi lines, which had a width of 254 μm. These patches appeared at different angles, which were positioned at 7°, 15°, 30°, 45°, 60°, 75°, 0°, and 90°.
3. Target 2C was comprised of the ultra-fine-line (21.17-μm width) patches at the same angles as the patches were positioned in Target 2B. The angled fine-line patch resolution was 150 lpi, while the horizontal (0°) and vertical (90°) patches in this target were specified at 120 lpi.

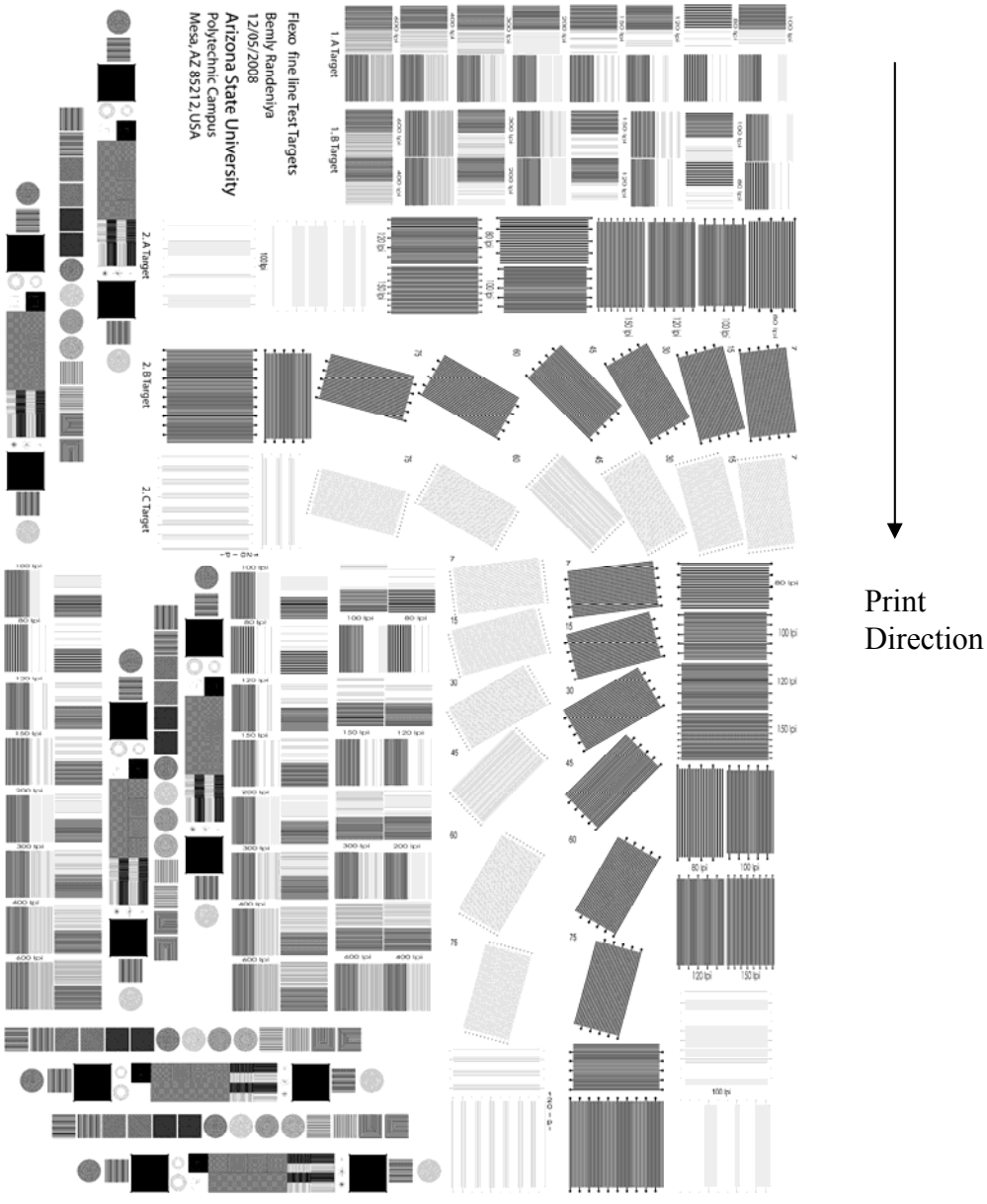

Figure 3. *Final Test Pattern Artwork with individual Targets 1A, 1B, 2A, 2B, and 2C.*

Microscopic evaluation of the flexo plate

The researchers realized the need to overcome the rounded tops and steep shoulders of the image, which traditional flexo plate frequently encounter. Rounded tops produce a mechanical value increase with higher impression pressures. The steep shoulders associated with small, narrower-line targets may cause less printing stability (and consequently more variability) while under higher impression pressure.

The Kodak NX flexo plate process was selected as the platemaking method. The digital Kodak Flexcel NXH imaging process is accomplished using a non silver-halide film to block the oxygen during the masking process to prevent rounded image tops from forming. A typical back exposure was used to set the floor height of the plate. The plate was processed in the Mekrom Processor using Solvit QD (from MacDermid) to remove polymer in non-image areas.

A Keyence VHX-600 Digital Microscope was used to evaluate and measure the flexographic plates and capture digital images. Two different lenses were used; the VH-Z20 ultra-small high-performance zoom lens, and a VH-Z100 wide-range zoom lens.

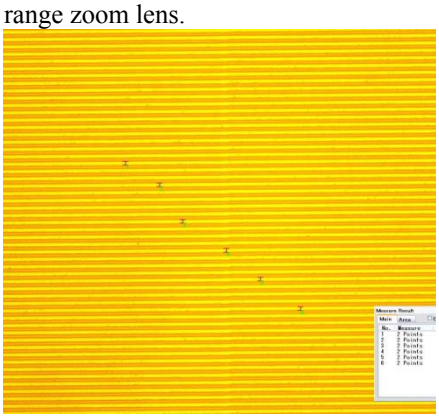

Figure 4. *10.58 mμ horizontal line (measured width 10.5 μm).*

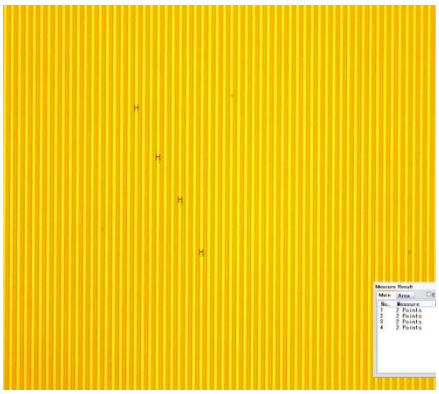

Figure 5. *10.58 mμ vertical line (measured width 9.6 μm).*

The lines were created at 2400-ppi resolution for flexo artwork. This means that one pixel equals 10.58 μm (1/2400 inches=10.58 μm).

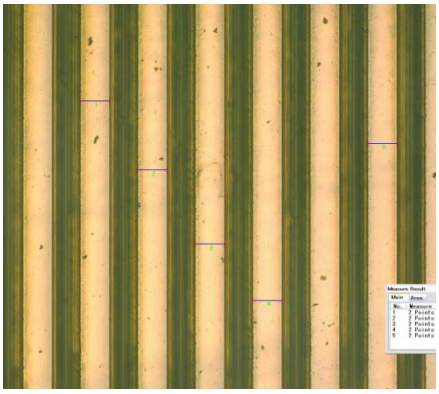

Figure 6. *169 µm vertical line (measured width 173 µm).*

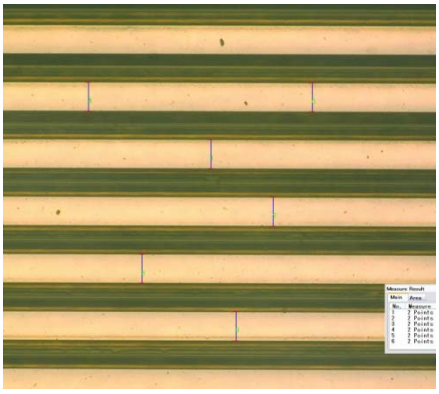

Figure 7. *169 µm horizontal line (measured width 172 µm).*

The figures above show the measuring properties of the 150-lpi vertical and horizontal lines. The average widths were recorded as 173 µm and 172 µm respectively. Other line widths also were similarly measured as indicated in Table B.

	Plate Widths (µm)		Theoretical Width (µm)
	Horizontal	Vertical	
80 lpi	318	318	317
100 lpi	255	255	254
120 lpi	212	214	211
150 lpi	172	172	169
200 lpi	124	125	127
300 lpi	82	83	84
400 lpi	61	62	63
600 lpi	38	40	42

Table A. *Actual line widths and theoretical line widths of Target 1.A (Flexography).*

2A	Plate Widths (µm)		Theoretical Width (µm)
	Horizontal	Vertical	
80 lpi	318	318	317
100 lpi	255	257	254
120 lpi	214	214	211
150 lpi	172	173	169

Table B. *Actual line widths and theoretical line widths of Target 2.A (Flexography).*

Microscopic evaluation of the gravure cylinder

The Schepers Digilas indirect laser engraving system was used for rotogravure cylinder preparation. A shafted cylinder was electroplated with copper, polished, and then coated with a resist. The resist was ablated using a laser and then chemically spray-etched to produce a precise cell pattern below the cylinder surface. After etching, the remaining resist was removed and the cylinder was cleaned using conventional methods.

Cylinders were then electroplated with a thin layer of chromium to ensure sufficient surface hardness to protect the copper layer against oxidation, possible scratches, and abrasion by the doctor blade used during the print run. The chrome thickness was verified at 0.0005-in. (12.7 μm), and the Chrome layer was cross-polished using a 3M lapping film (12 micron aluminum oxide coated on 1 mil polyester film).

The Tegatron CMD-IV microscope was used to inspect and measure the engraved gravure cylinder. A Mitutoyo SJ401 Surface Roughness Tester was used to evaluate the cell depths.

As in all gravure cylinder preparation processes, a screened cellular pattern was introduced into the artwork to produce cell walls. It was assumed that a continuous engraved line (without cell walls along the fine line) would populate more ink and cause ink spread-outs in printing due to nip pressure. Square and rectangle shaped screen patterns were used depending on the resolution and area. The gravure cylinder's face width was 13-in. and the circumference was 9-in. All the images were taken at 20X optical magnification.

The images of different resolution patches were named based on their orientation to the cylinder. In the naming convention, any line oriented so that it wrapped around the circumference of the cylinder is labeled "VERTICAL" while any line oriented so it runs with the axis of the cylinder is labeled "HORIZONTAL." In the printed sheet, the vertical lines were oriented towards the print direction while the horizontal lines were aligned in the cross-print direction.

Microscopic images of the horizontal and vertical lines at 100 lpi and 600 lpi are shown below.

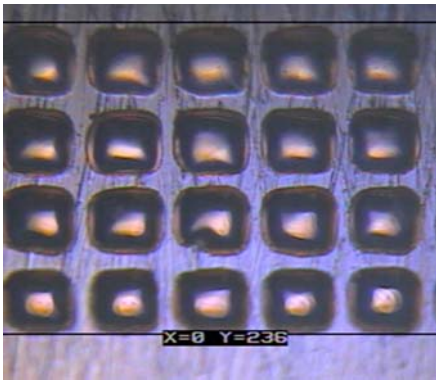

Figure 8. *254 µm horizontal line in 100 lpi (measured width 236 µm).*

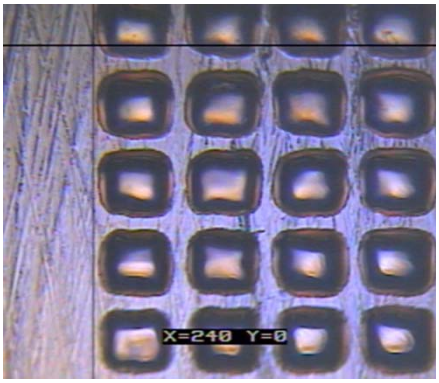

Figure 9. *254 µm vertical line in 100 lpi (measured width 240 µm).*

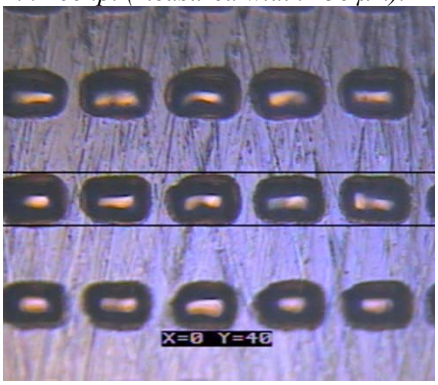

Figure 10. *42 mµ horizontal line in 600 lpi (measured width 40 µm).*

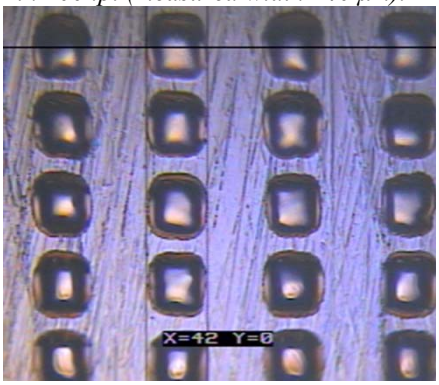

Figure 11. *42 mµ vertical line in 600 lpi (measured width 42 µm).*

1A	Engraving Width μm		Theoretical Width (μm)
	Horizontal	Vertical	
80 lpi	316	300	317
100 lpi	236	240	254
120 lpi	177	175	211
150 lpi	164	165	169
200 lpi	115	123	127
300 lpi	82	70	84
400 lpi	55	54	63
600 lpi	40	42	42

Table C. *Actual line widths and theoretical line widths of Target 1A .*

2A	Engraving Width μm		Theoretical Width (μm)
	Horizontal	Vertical	
80lpi	294	297	317
100lpi	230	237	254
120lpi	176	182	211
150lpi	162	164	169

Table D. *Actual line widths and theoretical line widths of Target 2A.*

Comparison of a specific location after exposure to laser imaging, etching, and chroming

A specific location of the cylinder image after the laser imaging, etching, and chroming stages was examined using the Tegatron CMD-IV digital microscope. The images below show the increase of the measurement in each step.

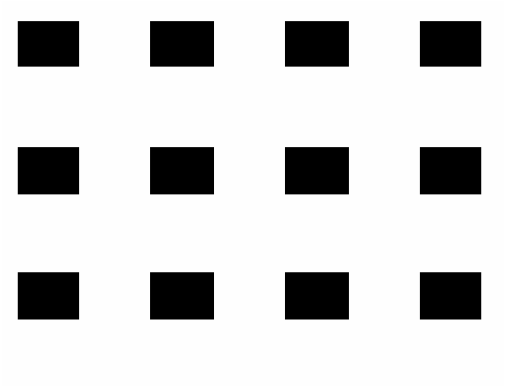

Figure 12: *Digital artwork (each image size 21μm X 16 μm).*

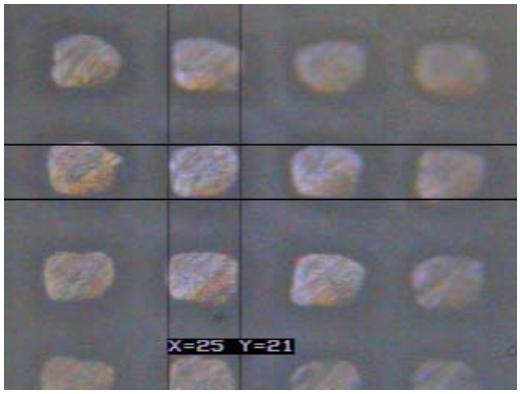

Figure 13. *After laser (cell size 25μm X 21 μm).*

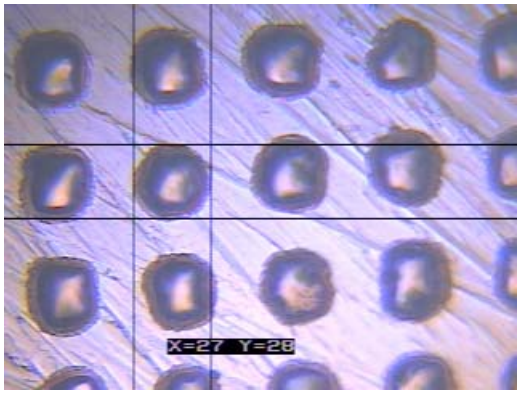

Figure 14. *Etched file (cell size 27μm X 28 μm).*

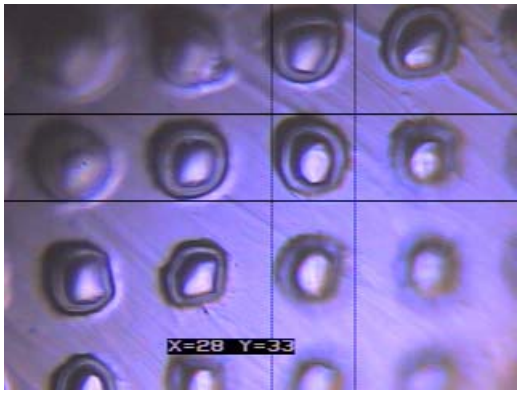

Figure 15. *Chromed file (cell size 33μm X 28 μm).*

Thermogravimetric Analysis (TGA)

Thermogravimetric analysis (TGA) is an analytical technique used to determine a material's thermal stability and its fraction of volatile components by monitoring the weight change that occurs as a specimen is heated. The measurement was carried out in air to find the carbon filler content of the ink as a percent of weight.

Two samples of Electrodag PE 003 carbon ink, weighing 7.081 mg and 8.713 mg respectively, were used to verify data accuracy. The minimal differences of the test data of two samples show that test results have been achieved with minimal errors. An ink sample was taken from the diluted PE 003 during the press run. The testing was performed at 10°C/min under an air atmosphere using a TA instrument model TGA 2950 HR. The weight is recorded as a function of increasing temperature, starting from 30°C to 600°C. Table E, and Figures 16

and 17 show the total percent of weight lost, onset of weight loss, and the different points of weight losses.

ID	Total Weight Loss %	Onset of Weight °C	Loss Rate Max Temp °C #1	Loss Rate Max Temp °C #2	Loss Rate Max Temp °C #3	Loss Rate Max Temp °C #4	Loss Rate Max Temp °C #5
PE-003 #1	88.98	42.92	69.18	252.09	334.08	426.19	572.52
PE-003 #2	84.43	49.90	73.64	270.39	322.11	418.00	579.46
Mean	86.71	46.41	71.41	261.24	328.10	422.10	575.99

Table E. *Total weight lost as a percent, onset of weight, and the different points of weight losses and their mean values.*

The two graphs for the two samples are displayed in the figures below. The green line indicates the total weight loss as a percent. The blue line indicates the rate of weight loss. The x-axis shows the time in minutes and the y-axis shows weight percent. The temperature in C° is graphed in green while the derivative weights are shown in blue. The derivative weight loss curve is the measurement of rate of weight loss with respect to time.

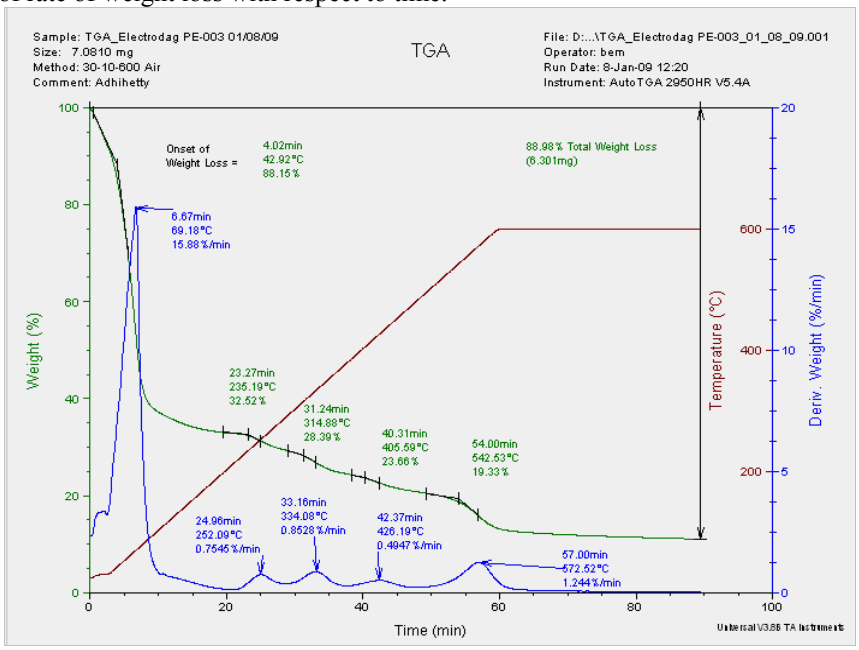

Figure 16. *Thermogravimetric graph of Sample 1 of PE003 ink.*

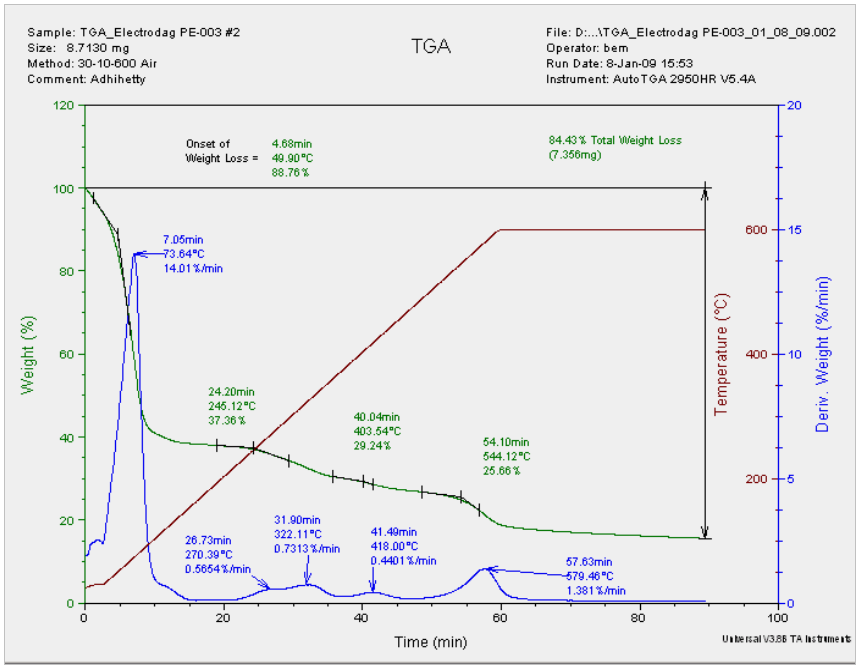

Figure 17. *Thermogravmetric graph of Sample 2 of the PE003 ink.*

Contact angle

The Young Relation describes the angle formed between a liquid and a flat horizontal surface. The solid interface to the surface specifically addresses the energy differential between the two. The measurement of this contact angle is useful for understanding the printability of both the substrate and the ink system.

The Drop Snake plug-in (http://bigwww.epfl.ch/demo/dropanalysis/) was used in the freeware Image J application (http://rsbweb.nih.gov/ij/index.html) to measure the static contact angle of PE 003, conductive carbon ink. Two microliters of ink for each of five measurements were taken for data accuracy. The contact angle was obtained by a piecewise polynomial fit using the Drop Snake method. The contact angle of PE 003 ink on Lusterprint GR2Max paper is 42° with an error tolerance of plus or minus 3°, which appears to be within expected limits for this test.

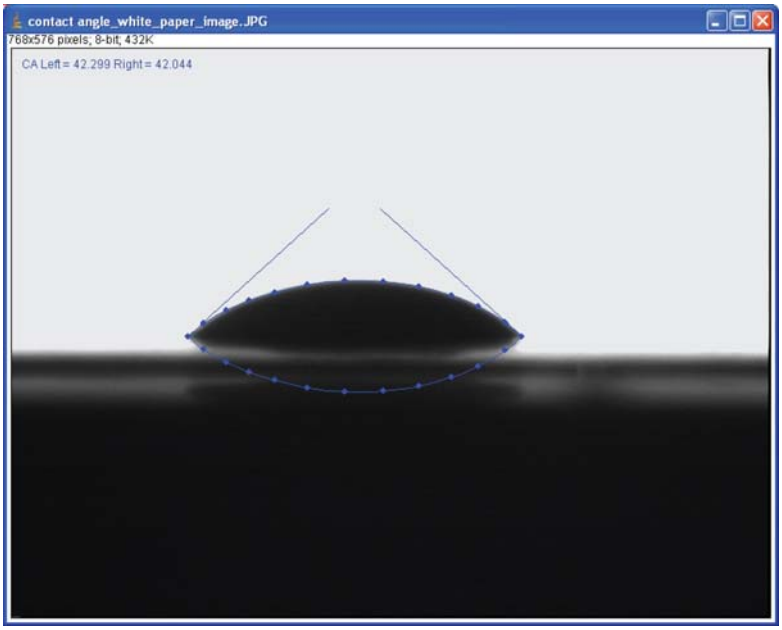

Figure 18. *Static Contact angle of PE 003 using Drop Snake plug-in in ImageJ freeware application.*

The contact angle may be defined as the angle made by the initial contact of the liquid with the solid surface of the substrate and the liquid-air contact point. It can be alternately described as the angle between substrate's surface and the tangent of the perimeter of the droplet's oval shape. High contact angles (which result in low degrees of wetting ability) would indicate low substrate surface energy, which can be interpreted as the lack of chemical affinity between the ink and the substrate. Low contact angles would indicate high substrate surface energy and indicate better chemical affinity between the ink and substrate. Contact angles near zero degrees will indicate complete chemical affinity and a more complete wetting of the substrate by the ink.

Surface tension and surface energy

Surface tension of a liquid is a measure of the intermolecular attraction between the liquid's molecules. High-surface tension liquids do not wet solid surfaces easily. Low-surface-tension liquids wet most solid surfaces because they generally exhibit higher intra molecular attraction. According to Gilleo (1996), a liquid will only wet a solid surface if the surface tension of the liquid is lower than that of the solid.

A variety of techniques exist to measure liquid surface tension. Determining the surface energy of a solid is more complex. The surface energy of a solid can be

calculated from a set of liquid/solid contact angles, developed by bringing various liquids in contact with the solid surface to be measured.

Using the Fowkes method, the effect of surface tension in ink transfer can be determined. Surface tension originates from an imbalance of attractive forces on a molecule at the surface. Close to the surface of a liquid, the molecules are separated and therefore have higher energy. In this experiment, the measurement of surface tension as performed by a Tensiometer is based on force measurements of the interaction of a probe with the surface of the interface of two fluids.

Figure 19 below shows the surface tension values in mili-Newtons/meter (mN/m) of the diluted PE 003 ink sample by the Wilhelmy plate method using a Kruss Processor Tensiometer model K100 with a standard thickness (19.9 mm x 0.2 mm) platinum plate. The standard deviation of surface tension values were calculated as 0.02.

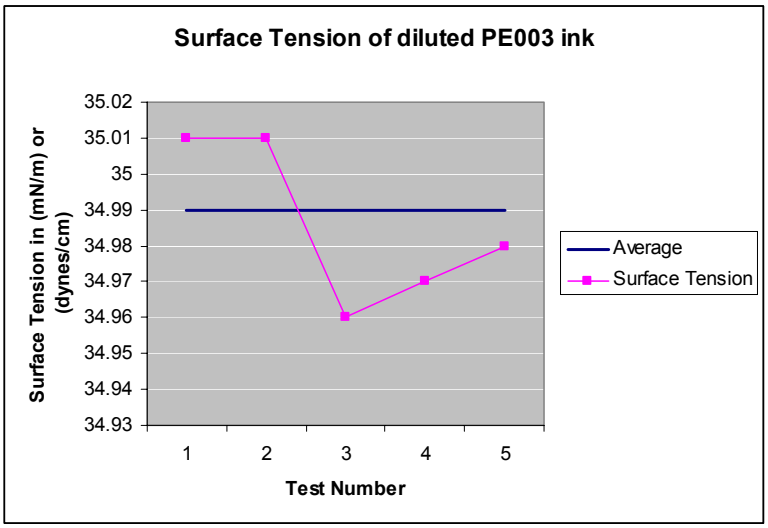

Figure 19. *Surface tension of PE 003 carbon ink.*

Table F shows values of surface energy of the Lusterprint Paper sample by the Fowkes method using water and diiodomethane as probe liquids. The following contact angles were measured for the probe liquids on the surface using 1.0 microliter drops with a Kruss Drop Shape Analysis System DSA100.

Drop	Water Contact Angle	Diiodomethane Contact Angle
1	68.8°	47.3°
2	69.0°	47.8°
3	69.4°	47.9°
4	68.9°	47.8°
5	68.8°	48.0°
Mean	69.0°	47.8°
Std. Dev.	0.2	0.3

Table F. *Contact angles of Water and Diiodomethane.*

Using the average contact angle values and the Fowkes theory, the surface energy components were calculated for the Lusterprint coated surface and are displayed in Table G.

Overall Surface Energy (mJ/m^2) or ($dynes/cm^2$)	Polar Component (mJ/m^2) or ($dynes/cm^2$)	Dispersive Component (mJ/m^2) or ($dynes/cm^2$)	Surface Polarity (%)
43.13	7.64	35.49	17.72

Table G. *Overall surface energy of the Lusterprint GR2Max substrate.*

Porosity and surface smoothness of the substrate

For most of the paper properties, it is more important to get information about paper voids than about the composition of the fibre in the paper. The porosity of the substrate (Lusterprint GR2Max paper) was measured using a Gurley Standard Manual Densometer. The densometer test measures the time required for a given volume of air (25 to 300 cc) to flow through a standard area of material being tested under light uniform pressure. Densometer readings are a direct test of materials, which are intended to either resist or permit the passage of air.

Surface smoothness was measured by the Sheffield method using Hagerty 538 Roughness Tester to indicate the degree of roughness for comparison. The results are displayed in Table H below.

Property	Instrument	Method	Test Result	Comment
Porosity	Gurley Densometer	Sec/100cc	0	No air transfer.
Surface Smoothness	Hagerty 538	Sheffield Units	95/213	

Table H. *Porosity and smoothness test results for Lustreprint GR2Max paper substrate.*

Gravure and Flexo Press Runs

Gravure press run

The Mark Andy 2200 flexographic press (13-in. narrow-web) had a gravure printing cassette on board and was employed to run the gravure test. The gravure printing cassette had two thermal curing units in position in the press. In this cassette, the maximum thermal output is approximately 210°F (plus or minus 5°F) at full capacity. However, for speeds of 50 fpm and 100 fpm press runs the curing operated at a lower capacity power level, while above 150 fpm press runs were running with the maximum thermal output.

A 60 Durometer impression roll and an enclosed ink chamber with lower blade as the metering doctor blade were used. The angle of the doctor blade in the relaxed state was 34° and it was set for 30° when under pressure (see Figure 20). Further, 65 pounds of force was calibrated on one actuator cylinder under applied air pressure by using a spring scale. With two air cylinders operating, the applied force on the chamber was calculated to be 130 pounds, at an air pressure of 22 psi. This pressure resulted in a total applied force to the ink chamber of approximately 130 pounds, and was applied to the gravure cylinder equally through the contact of both doctor blades. With only the lower blade engaged, it was assumed that the force between the gravure cylinder and the lower metering doctor blade was 65 pounds.

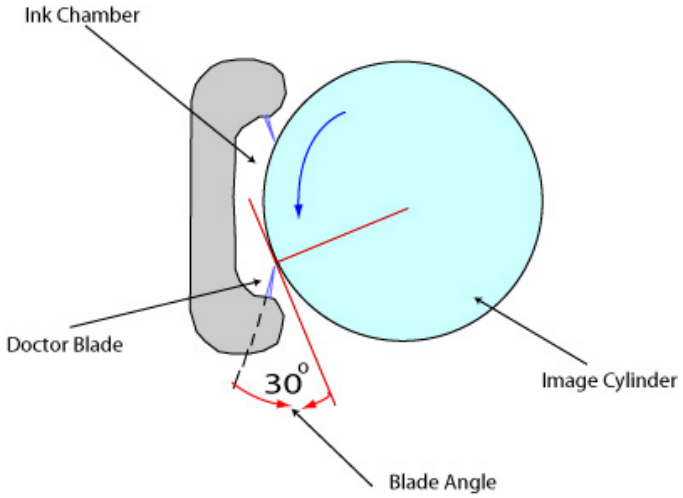

Figure 20. *Ink chamber with enclosed doctor blade in Mark Andy 2200 flexographic press.*

The gravure cylinder was positioned in the first unit of the press with counter-clockwise rotation. An S90 Zahn Cup (Number 2) was used to measure ink viscosity. On the ink manufacturer's recommendation, an equal amount of water and ammonia (NH_3) was used for dilution. The ink solution's viscosity was brought down to 24 seconds with the final pH value of 8.5. The initial pH values of water, NH3, and undiluted PE003 were measured as 9.7, 11.5, and 7.5 respectively. The print samples were collected at different speeds: 50, 100, 150, 250, and 500 feet per minute. The press room humidity and temperature were controlled at 23% and 75°F through the entire press run.

Flexo press run

The same press was employed for the flexo press run as well. However, the second printing unit was used in concert with a 6 bcm (billion cubic microns/in^2) anilox roller and ink chamber. The viscosity of the ink was reduced to 20 seconds using the #2 Zahn cup. In this instance too, the print samples were collected at different speeds: 50, 100, 150, 250, and 500 feet per minute. The press room humidity and temperature were also controlled at 23% and 75°F throughout the press run.

Gravure and Flexo Printed Line Evaluations

Gravure printed lines

As it was observed that the 500 fpm printed sheets' visual printed quality was better compared to the other speeds, it was decided to measure line widths on a sample printed sheet which was run at the speed of 500 fpm. The Keyence VHX-600 digital microscope using the VH-Z20 zoom lens was used to perform

this task. The optical zoom was set up at 100X when images were being captured. Images of different resolution patches for both directions, Print direction (PD) and Cross-Print direction (CPD) of Target 1A were initially captured to evaluate the visual quality.

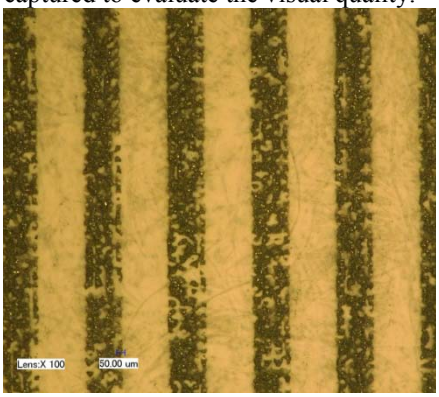

Figure 21. *Gravure printed lines, 100 lpi in the print direction.*

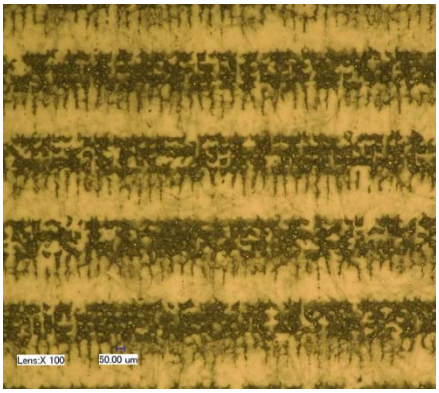

Figure 22. *Gravure printed lines, 100 lpi in the cross-print direction.*

It was clearly observed that the ink transfer from the gravure cells was incomplete. Many void spaces could be seen in the cross-print direction. Target 2A's 21-µm line in 100-lpi resolution patches also were captured.

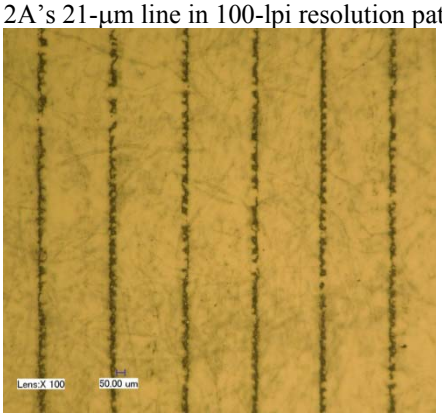

Figure 23. *Gravure 21 µm printed lines, 100 lpi in the print direction.*

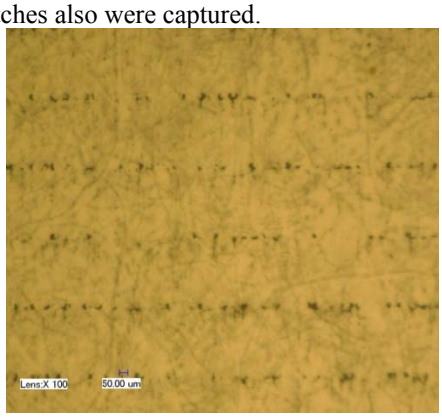

Figure 24. *Gravure 21 µm printed lines, 100 lpi in the cross-print direction.*

Images of the 21-µm line in 100-lpi resolution at both print and cross-print direction are shown above. The print-direction line print quality did not meet quality expectations. The cross-print direction line showed hardly any ink transfer.

Line widths of Target 2A's print directional and cross-print directional patches were measured using the Keyence VHX-600 to compare the theoretical width, engraving width and the printed line width.

Gravure Line Width (Print Directional) Comparison				
2A	Engraving Width (μm)	Theoretical Width (μm)	Printed Line Width (μm)	Deviation from Theoretical Width (%) (μm)
80 lpi	297	317	317	0.0
100 lpi	237	254	242	-4.7
120 lpi	182	211	193	-8.5
150 lpi	164	169	170	0.6

Table I. *Growth of the line width of gravure.*

Flexo printed lines

Similar to the gravure evaluation, it was decided to measure 500 fpm printed sheets. The Keyence VHX-600 was again used for this task. The optical zoom was set up at 100X when images were being captured. Images of different resolution patches for both directions, Print direction (PD) and Cross-Print direction (CPD) of Target 1A were initially captured to evaluate the visual quality.

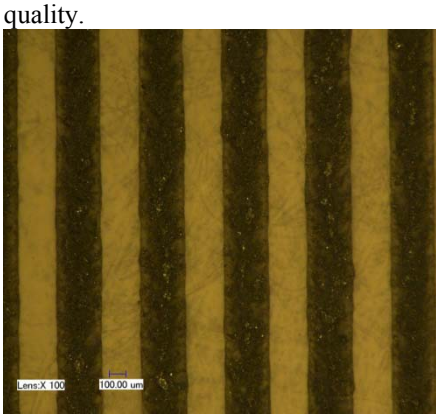

Figure 25. *Flexographic printed lines, 100 lpi in the print direction.*

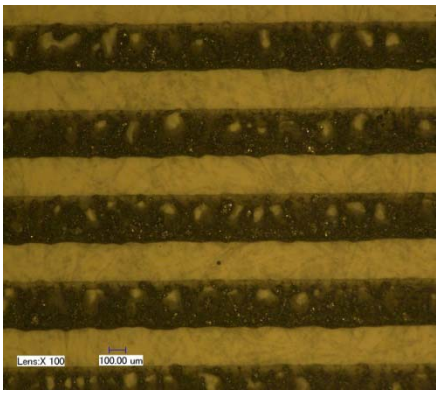

Figure 26. *Flexographic printed lines, 100 lpi in the cross-print direction.*

The 100-lpi images showed an acceptable print quality irrespective of print direction. However, cross-print direction shows some void spaces even though it does not affect the conductivity**.** Similar to the gravure evaluation, Target 2A's 21-μm line in 100-lpi resolution patches also were captured.

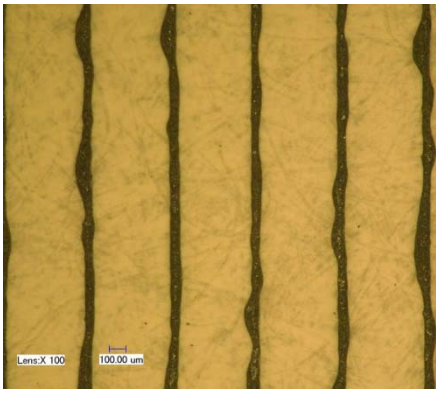

Figure 27. *Flexographic 21 µm printed lines, 100 lpi in the print direction.*

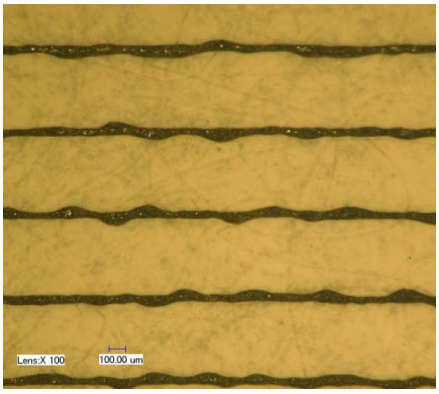

Figure 28. *Flexographic 21 µm printed lines, 100 lpi in the cross-print direction.*

A large mechanical growth of the printed line was seen in the 21-µm lines in 100 lpi. Strangely, the growth varied in position within the same line, irrespective of the print direction.

Similar to the gravure measurements, line widths of Target 2A's Print directional and Cross-Print directional patches were measured

2A	Flexo Plate Width	Theoretical Width	Printed Line Width in the Print Direction	Deviation from Theoretical Width (%)	Printed Line Width in the Cross-Print Direction	Deviation from Theoretical Width (%)
80 lpi	318	317	324	2.2	354	11.7
100 lpi	255	254	271	6.7	290	14.2
120 lpi	214	211	236	11.8	241	14.2
150 lpi	172	169	196	16.0	202	19.5

Table J. *Growth of line widths in flexo Target 2A in both print and cross-print directions.*

Gravure and Flexo Printed Line Conductivity

Conductivity in gravure

It was decided to collect a sample data set of 30 from each speed to perform a more meaningful statistical analysis. An IDEAL 61-495 PlatinumPro Data Logging Multimeter with a fine test lead was used to measure the resistance of lines in different resolutions and speeds. All line patches are one inch in length.

Resistances of lines aligned in print direction (PD) of Target 2.A and the angle 75° of Target 2B were collected as the Cross-print direction lines' resistances were not feasible due to poor print quality. The Resistances were measured in MΩ and plotted in Table K with respective standard deviations. Further, it was observed that higher line resolutions (120 lpi and 150 lpi) did not show any conductivity in the 50 fpm speed, thus are not recorded in the data.

Mean Resistance for Different Press Speeds in Gravure Target 2A					
Speed in Feet Per Minute (fpm)	80 lpi (PD)	100 lpi (PD)	120 lpi (PD)	150 lpi (PD)	Angle 75 to (CPD) of Target 2.B
500	2.65	3.4	3.54	4.95	3.86
250	3.96	4.01	4.9	5.18	6.6
150	4.37	4.93	5.13	6.63	8.26
100	4.89	4.48	5.77	6.3	8.39
50	5.92	6.48	N/A	N/A	N/A

Table K. *Mean resistance for different press speeds in gravure Target 2.A and angle 75° of Target 2.B.*
*(*PD= Print Direction and CPD= Cross-print Direction)*

Conductivity in flexo

In addition to the data gathered by the gravure process, the cross-print directional lines were also measured on the flexo press sheets. Further, it was possible to measure all angled line patches at 100 lpi resolution (Target 2B). The same IDEAL 61-495 PlatinumPro Data Logging Multimeter with fine test lead was used to measure the resistance.

Mean Resistance in MΩ for Different Press Speeds in Target 2.A of the Flexo Press Runs								
Speed	80 lpi (PD)	80 lpi (CPD)	100 lpi (PD)	100 lpi (CPD)	120 lpi (PD)	120 lpi (CPD)	150 lpi (PD)	150 lpi (CPD)
500 fpm	5.44	4.3	4.12	4.46	4.84	5.36	6.2	7.2
250 fpm	2.92	2.24	3.45	2.44	4.27	2.73	5.11	3.24
150 fpm	5.31	3.85	5.11	3.47	5	3.14	5.85	3.39
100 fpm	10.64	4.9	9.13	6.13	5.78	3.78	6.16	4.03
50 fpm	9.35	4.34	7.28	3.95	6.91	3.54	5.82	3.53

Table L. *Resistance for different press speeds in Target 2.A of the flexo press run. (*PD= Print Direction and CPD= Cross-print Direction)*

Mean Resistance in MΩ for Different Press Speeds in Target 2.B of the Flexo Press Runs								
Speed	7°	15°	30°	45°	60°	75°	0°	90°
500 fpm	2.49	4.12	4.54	4.38	4.11	4.74	4.42	4.6
250 fpm	2.83	3.27	3.05	2.91	2.15	2.28	3.55	2.1
150 fpm	3.43	4.74	3.28	4.35	3.81	4.29	4.1	2.87
100 fpm	6.24	6.1	3.79	4.31	4.2	4.6	4.79	3.2
50 fpm	4.83	3.99	3.14	3.03	2.31	3.15	6	2.72

Table M. *Resistance for different press speeds in Target 2.B of the flexo press run. (*Angles based on the print directional horizontal line)*

Ink Adhesion

Ink adhesion is most commonly measured with the tape test. Finished circuits are often checked with ordinary Scotch tape without cross-hatching since this gives a non-destructive test and many more circuits can be checked. In this experiment, ASTM standard Test D3330 Method B was carried out using Gardco PA 2000 cutting tool. First, solid patches of the 500 fpm speed gravure and flexo press sheets were cut through the ink film to the substrate in steady motion which created lines 1 mm apart.

DISCUSSION

Engraving and plate-making quality: gravure

When originally planned, the artwork for the test pattern was made at 2, 400 ppi, as required by the specifications for the flexographic plate-making process. Once produced, that same test pattern was re-sampled up to the 4,800-ppi resolution needed for the gravure cylinder engraving process, and then used that file to engrave the cylinder for the test. During this phase of the project it was noticed that, once the cylinder was engraved, the widths of the lines in the test pattern were reduced by the engraver to compensate for the expected mechanical growth that would normally be experienced by the gravure printing process. This may be attributed to the cellular pattern that was introduced onto the image during the prepress stage. Once printed, the line width returned to its approximately nominal state.

The theoretical line width of the artwork was calculated from the allocated pixels to the line. Since the gravure artwork was created in 4800-ppi resolution, one pixel was equal to 5.29 μm. Hence, the width of an 80-lpi line was calculated as 317 μm (5.29μm X 60 pixels). It was noted that at 120 lpi, lines of both Target 1A and Target 2A were considerably narrower compared to the theoretical width.

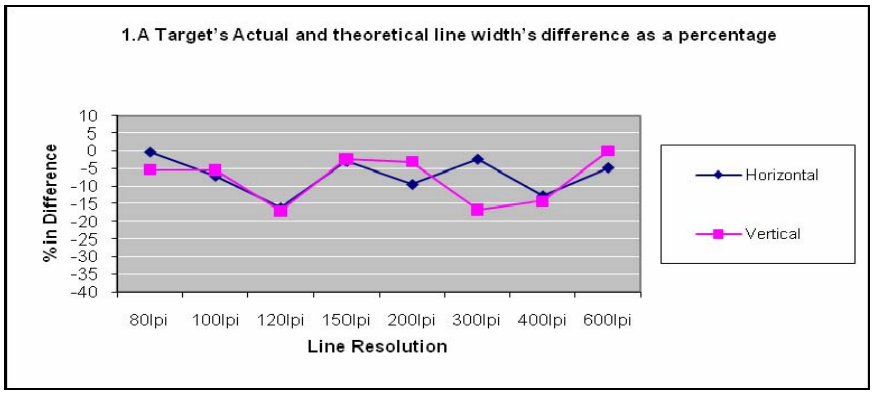

Figure 29. *Gravure Target 1.A's actual and theoretical engraving line width's difference as a percentage.*

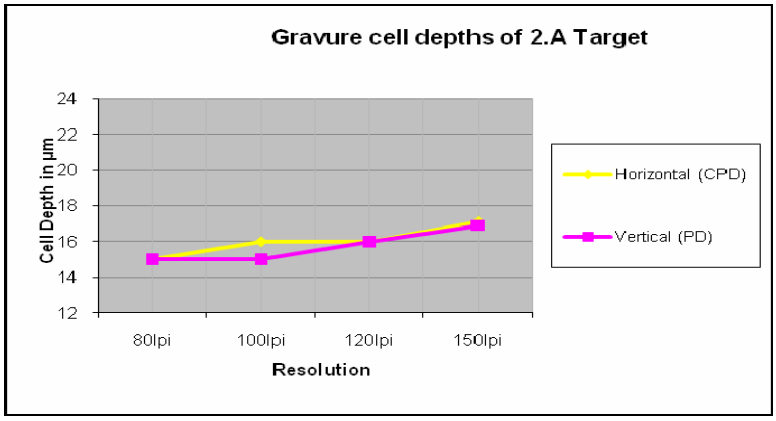

Figure 30. *Gravure Target 2.A's actual cell depths.*

Further, it was noted that in the Target 2A, vertical lines (lines that run in the circumferential direction) have a greater width in contrast to horizontal lines. However, this situation is not fully reflected in the Target 1A which had line patches in different resolutions, whereas the Target 2A only has lines in 100-lpi resolution. In general, vertical lines of both Targets were closer to the theoretical line width compared to other lpi counts.

It was observed that the usage of a cell structure on fine lines is to be done very cautiously. If the cell pattern falls with 1px (in any resolution) line in the digital artwork, this may give a different image or lines may not be imaged at all. This may be critical in fine-line circles as the screen grid often appears as horizontal and vertical lines.

Figure 31 below shows incomplete cells in the upper horizontal line.

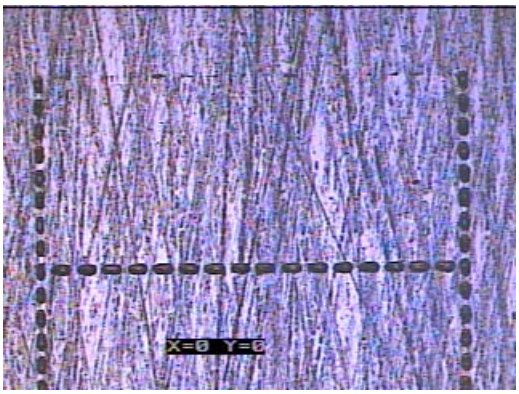

Figure 31. *Gravure image inconsistency cause by a screen pattern.*

Engraving and plate-making quality: Flexo

Table A and Table B revealed that Target 1A and Target 2A have insignificant variations in plate making in contrast to respective theoretical widths. The Kodak Flexcel NXH imaging process showed good consistency levels in the plate-making process, apart from some minor inherent defects which are described below. Lamination forces intimate contact between the Thermal Imaging Layer and plate to ensure 1:1 image transfer onto the plate. The Thermal Imaging Layer is specially constructed so that oxygen barriers effectively prevented oxygen from being present at the plate surface, eliminating oxygen inhibition as a variable. If oxygen were present, we could expect to see a bullet-shaped dot structure and inconsistent dot height. Eliminating these effects produced stable, full-height dots with flat tops. The observation of minimal variance in plate-making may be due to the minimizing of "oxygen inhibition" during UV exposure as well as the method of contact.

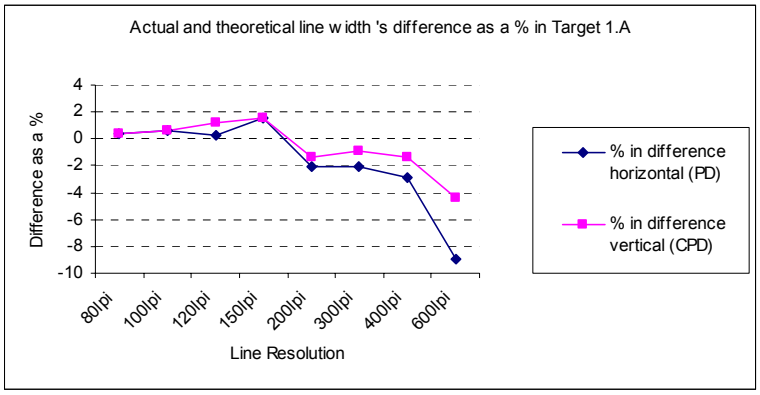

Figure 32. *Actual and theoretical line width differences as a % in Target 1.A showing both print directional (PD) and cross-print directional (CPD).*

Thermogravimetric analysis

As described, the thermogravimetric test provides an analysis of the carbon filler content of the ink as a percent of weight. Electrotag PE-003 ink, diluted with water and Ammonium Hydroxide (NH_4OH), exhibited an average total weight loss of approximately 87%, along with an onset of weight loss approaching 46°C. For example, a 10-mg PE 003 ink sample will contain 1.3 mg of the filler. The filler in this sample is carbon, which acts as the conductor since the evaporated component (8.7 mg) is comprised of non-metallic molecules. This material exhibited five weight loss regions with rate of weight loss maxima near 71°C, 261°C, 328°C, 422°C, and 576°C. A review of the thermograms suggests that the initial weight loss is due to curing, while the remaining weight loss regions suggest the occurrence at several thermally localized decompositions. The final observed weight loss region may be attributed to a final decomposition. Further, the results show that the filler content of the PE 003 diluted ink solution can be derived as 13% since the total weight loss was 87%.

Porosity and surface smoothness

The Sheffield smoothness test measures the amount of air that escapes when a Smoothness tester is pressed flat against the paper and air is blown out. The less air that escapes, the smoother the paper. The reading shows that the coated side of the paper is much smoother than the uncoated side. Smoothness is a surface characteristic relating to the flatness of a sheet, which affects its ink receptivity. It can be described that the smoother the sheet, is the sharper the image. However, substrate smoothness requirement is less critical in flexo than in the gravure process. A Sheffield value of 30 or less provides a surface that is sufficiently smooth for current flexographic printing (Gamota, Brazis, Kalyanasundaram, and Zhang, 2004). The Lusterprint's smoothness values (95 Sheffield units) are not very feasible either for gravure or flexo. The test data shows that the substrate has no air permeability (no air transfer through sheet), which is an important factor of substrate parameters. However, testing revealed that the employed substrate was not an ideal substrate for fine-line printing in terms of smoothness values.

Printed line quality—Gravure

The decision to include two levels above the 100 lpi (120 lpi and 150 lpi) and one level below (80 lpi) was productive as all four resolution patches were printed perfectly on the print direction (PD) with reasonable conductivity. However, none of the targets that were aligned in the cross-print direction (CPD) was acceptable since printed line discontinuations (breaks) were observed. The continuity of a printed line is paramount in printed electronics as it verifies the proper electrical transmission. Angled lines in 100 lpi in Target 2.B also were not satisfactory. Only the 75° angle (from the cylinder axis) showed adequate conductivity. Very fine line (20 μm) in 100-lpi and 150-lpi angle lines also had a poor print quality. While gravure is typically associated with high print quality and low variation throughout the print run, the print

quality can be adversely affected by a variety of factors, such as the substrate, the cylinder, the engraving quality, doctoring, and ink viscosity (Gamota, Brazis, Kalyanasundaram, and Zhang, 2004). Further, the cellular screen pattern also may have an impact on the proper engraving process that then translates into the print. Instead of rectangular-shaped screen, a diamond-shape screen pattern would have made a difference especially in the fine-line resolutions.

The positive indication of these results is that gravure process has a minimal growth in printed lines which is crucial factor in fine line printing.

Printed line quality—Flexo

Printed line quality is affected by many factors in the flexographic process, including artwork, substrate, plate manufacturing quality, anilox roll, and press conditions such as impression pressure and speed. Visual quality was acceptable except for the patches that were in the resolution of 300 lpi and above in Target 1A and Target 1B. It was clearly noticed by microscopic evaluation that the ink formation in printed lines is different from the print direction to the cross-print direction. In the print direction, the ink deposit is perfectly centered, while in the cross-print direction the images show that the ink seems to be deposited somewhat thicker towards the edge. The ink releasing side has less ink density compared to the opposite side of the line (see Figures 33 and 34).

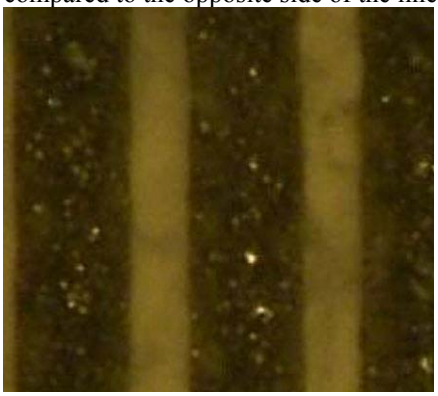

Figure 33. *A magnified view of the print directional line (300 lpi).*

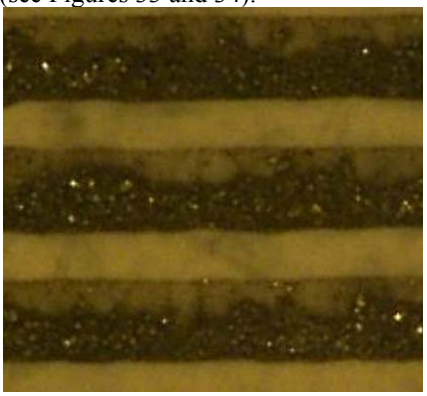

Figure 34. *A magnified view of the cross-print directional line (300 lpi).*

For an encouraging note, the finest line (21 μm) in 150-lpi resolution is printable in different angles. However, the widths of the same fine line were varied drastically in different locations (see Figures 27 and 28). It was noted that most variations were occurred in the print direction in contrast to the cross-print direction.

During the flexographic plate-making process, the expected mechanical growth in line width was not compensated for automatically. After printing the target

for the flexo part of the test, we noticed that the mechanical growth inherent in the flexo process had increased the line width of the test pattern.

The main concern of the flexographic process in terms of printed electronics is the higher degree of mechanical growth in the width of the printed line. It is revealed that a maximum of 16% growth was recorded on 150-lpi lines in the print direction while a 19.5% maximum growth was recorded on the same line in the cross-print direction. As expected, it was noted that the growth increased when the resolution was increased (as the line width decreased), in both the print direction and the cross-print direction. Similarly, as expected, the cross-print directional growth was recorded as higher when compared to the print directional lines.

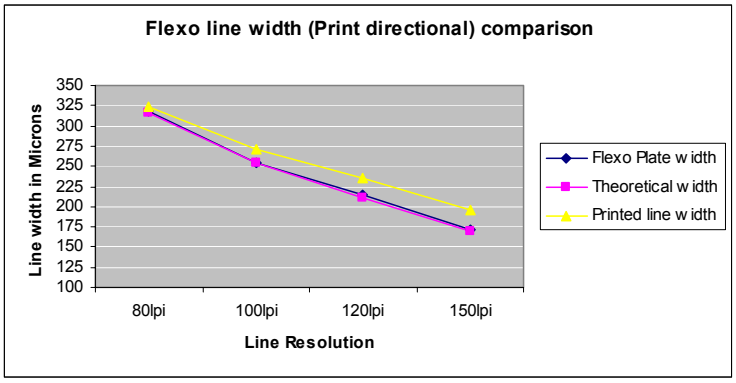

Figure 35. *Flexo line width comparison in Target 2.A (print direction).*

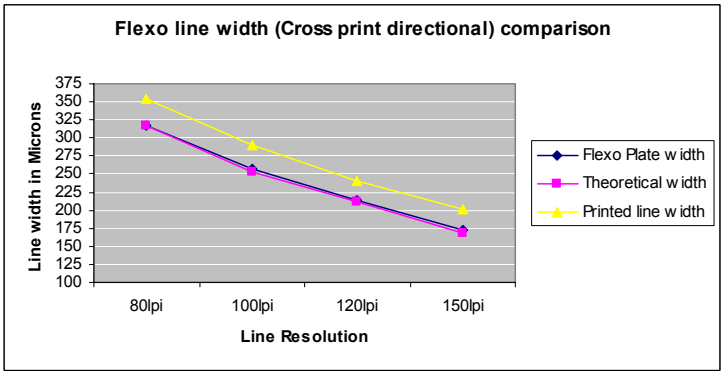

Figure 36. *Flexo line width comparison in Target 2.A (cross-print direction).*

Figure 35 and Figure 36 show a clear deviation of the printed line width from the plate and theoretical width irrelevant to its print direction. However, as described in the plate and cylinder evaluation section, plate widths and the theoretical width show minimal variation.

Printed line's conductivity in gravure

The electrical resistance of carbon is much higher than silver. The end-to-end measuring of the conductivity in gravure printed lines was comparatively high in terms of industry requirements. When measuring the lines in the target, it was determined that there was a trend toward increasing resistance that seemed to correlate with diminishing printing press speed. That is to say that the more the press speed slowed, the more resistance increased in the printed line. This trend was also observed as resolution increased. In other words, as the thickness of the line decreased, the resistance increased accordingly. The printed line quality and the low resistances were recorded at the speed of 500 fpm. At 50 fpm, the line widths increased due to mechanical growth to the point where the individual lines at finer resolutions blended together, and thus were no longer discrete traces in a circuit. As referred to above, this may be influenced by the fact that the curing section of the press was only capable of operating at half capacity at slower speeds and only went to full capacity at speeds over 150 fpm. More research is needed to determine this point.

As expected, as the line resolution increased, the thickness of each discrete line decreased, and resistance increased accordingly. We attribute this to the reduction of the cross sectional area of the conductive printed line.

Printed line's conductivity in flexo

The flexo process provided conductivity data for both Target 2A and 2B. In Target 2B, it was possible to measure the resistance in the cross-print direction as well.

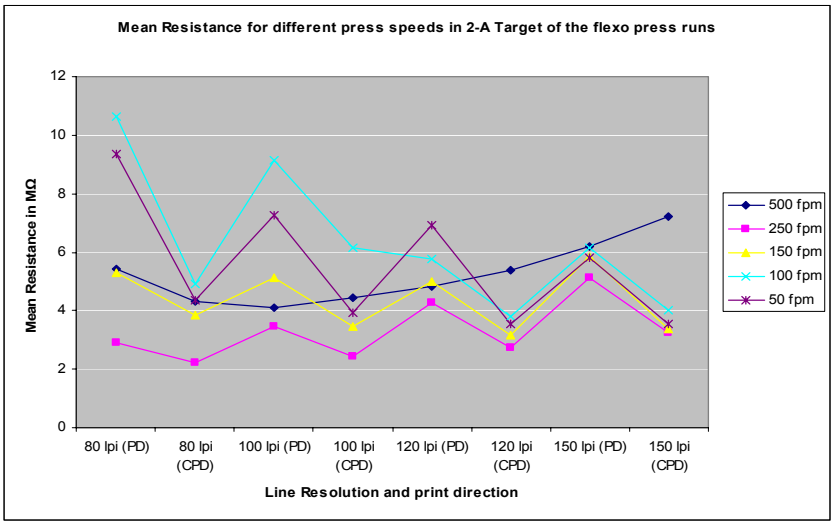

Figure 37. *Resistance for different press speeds in Target 2A of the flexo press run.*

The researchers expected that increases in press speed would result in approximately linear increases in resistance. Unexpectedly, while the 50-fpm speed resistances were high, the 100-fpm resistances (which were the highest of the tested speeds) were higher yet. The lowest resistance range was recorded at a speed of 250 fpm in all the available resolutions, in both the print direction and the cross-print direction. This was a curious phenomenon as data does not point directly to an answer. More study is needed to resolve this anomaly.

Between the speeds of 150 and 250 fpm, it was observed that increasing the press speed reduces the resistance. It was also observed that the cross-print directional resistance is lower as compared to the same resolution lines aligned in the print direction. This may be due to the larger width of the printed line in cross-print direction in contrast to the print direction. This observation does not apply to speeds in the 500 fpm range. It was also observed that the cross-print directional lines of the flexo press were wider than the print directional lines. This may be due to the effect of grain direction of the paper, which also runs parallel to the print direction.

Contact angle, surface tension, surface energy, and adhesion

A phrase usually mentioned in the printing industry is *low wets high.* This can be identified as the low surface tension or surface energy of the ink wets the substrate adequately, as long as the substrate's surface energy is higher than that of the ink's. The single-fluid ink used in the gravure process needs to be sufficiently fluidic to fill the cells entirely. Therefore, the ink must have a sufficiently low surface tension to wet the gravure cells. Furthermore, it needs to be low enough in viscosity to flow into and out of the cell again, and onto the substrate. The surface tension of PE 003 carbon ink was measured as 34.99 dynes/cm (mN/m).

This can be described as a low surface tension compared to water, 72 mN/m (or dynes/cm). The PE 003 ink was diluted enough to have a viscosity of 22 seconds in Zahn Cup 2. However, surface tension of the ink itself cannot determine a proper wetness of the gravure cell. It also depends on the surface energy of the gravure cell which is beyond this experimental scope. The surface energy of the substrate was measured and recorded as 43.13 dynes/cm^2. A high surface energy has a strong intramolecular attraction and is readily wet by most liquids. Generally, a substrate having a surface energy less than 40 dynes/cm^2 is very difficult to print on (Gamota, Brazis, Kalyanasundaram, and Zhang, 2004) since its intramolecular attractions are too small. Lusterprint substrate's recorded surface energy, 43.13 dynes/cm^2 seems somewhat low. The researchers were of the opinion that a surface energy of at least 50 dynes/cm^2 would have been better for this experiment for a quality print. If the droplet contact angle with the substrate surface is greater than 90°, the liquid tends to form droplets on the surface. If the contact angle is less than 90°, the liquid tends to spread out over

the surface and more easily wets the substrate. The contact angle of PE 003 which was measured as 42° was in the acceptable range in terms of wetting the surface.

PE 003 carbon ink was water-based and the curing was achieved with forced hot air. The measuring adhesion on tape test was very hard to perform as most of the time 100% of the area with the coated layer also was removed with the tape. A 25–35% removal both in gravure and flexo was the aim point of the experiment, which is needed to determine the amount of curing necessary for better adhesion. It is also known that the surface tension, surface energy, and adhesion are all interrelated. More research is needed to decide the effectiveness of the curing data for subsequent experiments.

Gravure vs. Flexography

Both processes showed adequate capacity to print relatively wide conductive lines. However, both processes have experienced considerable difficulty in printing ultra fine lines (20 μm) with proper conductivity.

Printed lines

Experimental data revealed that both Targets 2A (Table L) and 2B (Table M), were printable with minimal conductivity using the flexographic printing process. However, only Target 2A was printable with adequate conductivity with the gravure printing process. The main advantage that the gravure process has over flexography is the lower amount of mechanical growth of the printed lines (see Table I).

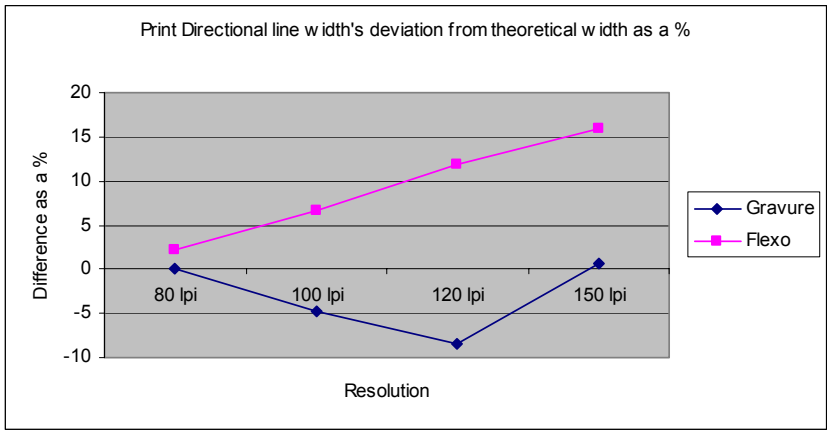

Figure 38. *Print directional line width deviations from theoretical width as a % (Gravure vs. Flexo) Line Chart.*

Figure 38 clearly shows that the gravure process exhibits lower levels of deviation from the theoretical width in respective resolutions.

Conductivity

Experimental data does not indicate a significant pattern related to comparisons in conductivity. However, the gravure process indicates a decline of resistance with increases in the press speed. The lowest resistance recorded in flexo is at 250 fpm while in gravure it is at 500 fpm (see Figure 39). Recording a lower resistance at a higher press speed can be considered a significant advantage in the gravure process, if other problems in cross-directional line conductivity can be successfully resolved.

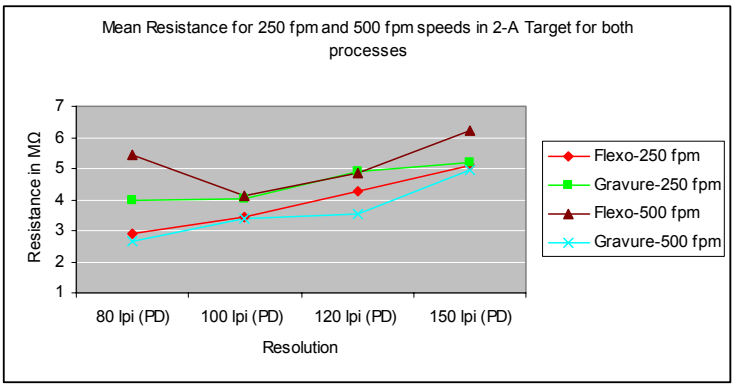

Figure 39. *Mean Resistance in MΩ for 250 fpm and 500 fpm speeds in 2.A Target for both processes.*

Engraving and Plate Making

Engraving and plate making

Engraving and plate-making differences were calculated. As part of the engraving process, the cell structure grid had to be recalculated for these test patterns so as to ensure that the cell structure of the lines didn't cause the lines to take on jagged-edge characteristics and to prevent the thin lines running circumferentially from becoming a solid, unending cell without land area to support the doctor blade at the surface of the cylinder. As a result, the researchers discovered that the effect of this recalculation unexpectedly reduced the thicknesses of the lines that were engraved in the test patterns. Thus, when printed, the resulting line thickness of the test patterns printed using the gravure process did not match the theoretical thickness computed for the lines in the test patterns. Further, the thickness of certain printed lines from the gravure test patterns did not prove to equal the same lines from test patterns printed with the flexographic process. It was assumed that this was due to the flexo plate-making process not compensating for mechanical growth and consequently printing

thicker lines in these test patterns. See Table I for the comparison between actual and theoretical line thicknesses.

Therefore, a significant (but acceptable) difference was observed with gravure. The flexo plate was created with minimal deviation from the theoretical width (see Figure 40).

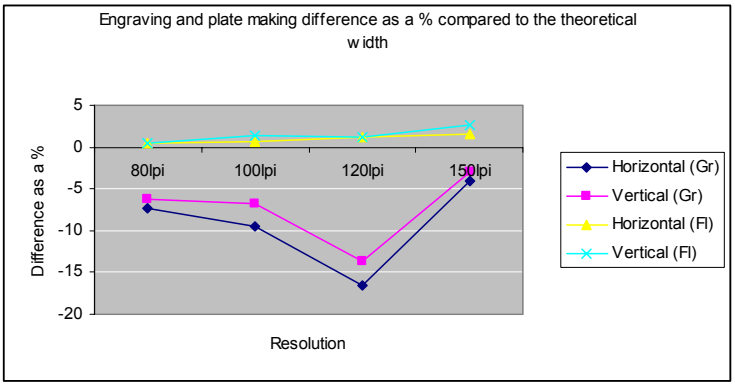

Figure 40. *Engraving and plate making differences as a % compared to the theoretical width.*

CONCLUSIONS

Summary

Both processes have shown some promise in their respective capabilities to produce printed electronic products. Both are mechanically straightforward processes in terms of accurately transferring the printed image to substrates. The flexographic process has a simple plate-making and plate-changing process, enhanced by its low plating costs. Gravure is a permanent master worthy of consideration so long as the graphic design on the engraved cylinder doesn't change often or quickly. Both processes have shown their capacity to print relatively wide conductive lines, and both processes have their own difficulties with printing ultra-fine-lines with proper conductivity.

Gravure

1. Considering very-fine-line printing, the engraving process plays a critical role in the quality of the reproduction. Cell-size optimization must be done carefully as the prediction of cell area and volume that is produced by chemical etching of the copper cylinder surface requires great skill.

2. It was relatively easy to achieve conductive printed lines (traces) which were equal to or wider than 150 μm, but it was much more challenging

to print finer lines having widths of 20 μm to 30 μm with reasonable conductivity. The problem lies not with optical quality, but with conductivity.

3. It was possible to print 150 lpi (75 lpi compared to optical printing terms) resolution traces (~ 170 μm width) in the circumferential (print) direction.

4. There were significant print quality differences between the print directional traces and the cross-print directional traces.

5. The cross-print directional print quality was considerably lower as compared to the print directional lines.

6. It was observed that the resistance of conductive lines gets lower as the press speed is increased, resulting in higher conductivity in those traces. It is an encouraging sign from the perspective of the gravure process.

Flexography

7. Conductive traces printed with the flexography process showed the capability of cross-print directional lines with reasonable conductivity.

8. It was observed that the digital artwork information was transferred to the plate with negligible variation, very desirable in the flexographic plate-making process. The plate-making of the flexographic process is quite acceptable in terms of producing an ultra fine line image. The plate-making process maintained a mere 2.63% deviation from the intended width.

9. The mechanical growth of the printed fine lines is relatively high in flexography, but during the plate-making process, no attempt was made to compensate for the mechanical growth of the lines.

10. It was possible to print 150 lpi (75 lpi in printing terms) conductive traces (~ 170 μm width) in both the print direction and the cross-print direction.

11. The cross-print directional lines indicated a higher amount of gain in mechanical growth, while the print directional lines didn't gain as much. However, the cross-print directional growth was found to be nearly within acceptable limits.

12. Even though the flexographic process produced the finest lines optically (21 μm) printable at 150 lpi, these lines produced almost no

conductivity when tested, due to frequent breaks in the ink film of the ultra-thin printed line.

RECOMMMENDATIONS

1. In order to determine a possible relationship between the gravure cell depth, cell opening, and the etching time to predict the fine-line width with desired depth, further study is needed.

2. The printed line quality and the lowest resistances of the gravure printing process were recorded at the speed of 500 fpm. Only 80 lpi and 100 lpi line resolution printing with conductivity was possible at speeds of 50 fpm. This may be due to the lower thermal curing output in the press due to the automatic control settings at lower press speeds. Again, the researchers believe that more study will pay dividends in determining the definitive cause of this problem.

3. When engraving the gravure cylinder, the researchers noticed that the sizes of the fine-line widths were reduced during the engraving process. This was also recorded during printing. On investigation, it was discovered that the engraver was set to reduce cell widths in compensation for expected mechanical growth of cell-generated halftone dots. In the print media, this is commonly called a TVI curve. Once applied, the researchers realized that they had made a change to the gravure process that wasn't made to the flexographic plates. This may have affected the results of the experiments and may be partly responsible for the shift in fine-line resistance at faster printing speeds, displayed in the gravure test but not the flexo tests. More research is needed to determine whether this was an un-accounted factor in the outcome of the experiment.

4. When attempting to measure ink film thickness, the researchers noted that the surface plane of the Lusterprint Max varied substantially, due in part to the grain pattern in this substrate. Due to this variance, the researchers were unable to get accurate ink film thickness data from the tests conducted. Therefore, it is recommended to conduct more research by printing the test pattern on a substrate that has less planar variability, such as PET or OPP so that accurate ink film thickness may be determined.

Acknowledgments

The authors would like to thank all those who have helped in numerous ways to accomplish this paper. This research would not be a reality without Mr. Mark

Richter, President, and Mr. Micheal Stava, Technical Manager, of RotaDyne Decorative Technologies Group, Ohio; Mr. Kevin Manes, Manager-R&D of Mark Andy Inc., Missouri; Mr. Gregory Zwadlo, Senior Scientist of Kodak Flexcel Group; Mr. Al Vega, VP Sales of Sappi Fine Paper North America; Dr. Indira Adihetty and Mr. Brian Moreira of Freescale Semiconductors; Dr. Christopher Rulison, Principal Scientist of Augustine Scientific, Ohio; Mr. Bob Arriola, Technical Manager of Neenah Paper; Mr. Reuben Rettke, Senior Color Scientist, NthDegree Technologies; Mr. Doug Gasser, Account Manager of Xpedx; Mr. Walter Siegenthaler, Executive Vice President of Max Daetwyler Corp.; Mr. Dan Fenner and Mr. Dave Shanta of Acheson Colloids; Dr. Thomas E. Schildgen, Professor, Arizona State University; Mr. Joseph Tissera, Chief Innovation Officer of Associated Newspapers of Ceylon Limited, Sri Lanka; Mr. Jeff Reimer, Software Engineer of Ticketmasters; and Mr. James A. Workman, Vice President, Training and Mr. Eric L. Newmann, Research Manager of Printing Industries of America.

The authors highly appreciate of their voluntarily support.

References

Blayo and Pineaux. 2005. "Printing Processes and Their Potential for RFID Printing." *Joint OC-EUSAI Conference Proceedings,* Grenoble SU

Bock, et.al. 2005. "Polymer Electronic Systems." *IEEE Proceedings 93*.

Falchetti. 2007. *Materials Today Asia Proceedings*, #10.

Gamota, R.D., P. Brazis, K. Kalyanasundaram, and J. Zhang, J. 2004. *Printed Organic and Molecular Electronics,* Massachusetts: Kluwer Academic Publishers, pp. 695.

Gilleo, K. 1996. *Polymer Thick Film*, New York: Van Nostrand Reinhold.

Gravure Process and Technology. 2003. Rochester, New York: Gravure Education Foundation. pp. 05.

Gupta, R.K. (2000). *Polymer and Composite Rheology*. New York: CRC Press.

Hagberg, J. M. Pudas, S. Leppävuori, K. Elsey, and L. Alison. 2001. "Gravure offset printing development for fine line thick film circuits." *Microelectronics International* : Volume 18 Number: 3 pp: 32–35.

Harrey, et al. 2000. "Sensors and Activators." *Journal of Electronics Manufacturing,* vol. 19.

Moore, G. 2004. “Paper-based products bloom.” BNET: Retrieved on October 2, 2008 from http://findarticles.com/p/articles/mi_qa5371/is_200411/ai_n21362307/pg_1?tag=artBody;col1

National Research Council. 2005. Linkages—*Manufacturing trends in electronic interconnection technology*. Washington D.C.: The National Academies Press.

Sheets. 2004. “Microphage Particle Interaction.” *Journal of Material Research,* vol. 19.

Vardeny. 2005. “Fundamental Research Needs in Organic Electronic Materials,” *Synthetic Materials,* vol. 148.

Xu, J.M. 2000. “Plastic Electronics and Future Trends in Microelectronics.” *Synthetic Metals,* vol. 115.